eng

MDPI

Article

A Human Self-Locking Cone Morse Connection Retrieved After 30 Years: A Histological and Histomorphometric Case Report

Carlo Mangano [1], Margherita Tumedei [2,3], Adriano Piattelli [4], Francesco Guido Mangano [5], Tea Romasco [6,7], Natalia Di Pietro [6,7,*] and Giovanna Iezzi [6]

[1] Department of Dental Science, Vita and Salute San Raffaele University, 20132 Milan, Italy; camangan@gmail.com
[2] Department of Biomedical, Surgical and Dental Sciences, Università degli Studi di Milano, 20122 Milan, Italy; margytumedei@yahoo.it
[3] Fondazione IRCCS Ca'Granda Ospedale Maggiore Policlinico, 20122 Milan, Italy
[4] School of Dentistry, Saint Camillus International University for Health Sciences (Unicamillus), 00131 Rome, Italy; apiattelli51@gmail.com
[5] Department of Prevention and Communal Dentistry, Sechenov First State Medical University, 119991 Moscow, Russia; francescoguidomangano@gmail.com
[6] Department of Medical, Oral and Biotechnological Sciences, "G. d'Annunzio" University of Chieti-Pescara, 66100 Chieti, Italy; tea.romasco@unich.it (T.R.); gio.iezzi@unich.it (G.I.)
[7] Center for Advanced Studies and Technology (CAST), "G. d'Annunzio" University of Chieti-Pescara, 66100 Chieti, Italy
* Correspondence: natalia.dipietro@unich.it

Abstract: The Cone Morse (CM) implant-abutment junction is designed to improve screw mechanics and minimize bacterial leakage through a process known as "cold fusion". This research evaluated a clinically stable self-locking CM implant that was retrieved after 30 years of functional loading, focusing on the bone–implant interface. Histological evaluation was conducted to assess the extent of bone-to-implant contact (BIC), identify any tissue reactions, and determine the overall condition of the interface. The analysis revealed a high percentage of BIC in the endosseous portion (56.9%) and at the first contact point (77.4%). Notably, the bone in direct contact with the implant showed healthy integration, indicating no signs of adverse reactions or degradation despite the long duration of functionality. Additionally, osteocyte lacunae were found to be more numerous and larger in the coronal region compared to the apical region. These findings confirmed that the CM implant design sustains a high degree of BIC in humans, even after extended functional loading. The absence of epithelial migration, inflammatory infiltrate, and fibrous tissue at the interface suggests that this type of implant can offer long-term stability and integration.

Keywords: bone-to-implant contact (BIC); Cone Morse implant; histological analysis; implant stability; long-term functional loading; osseointegration

check for updates

Academic Editor: Leszek A. Dobrzanski

Received: 1 February 2025
Revised: 6 March 2025
Accepted: 18 March 2025
Published: 20 March 2025

Citation: Mangano, C.; Tumedei, M.; Piattelli, A.; Mangano, F.G.; Romasco, T.; Di Pietro, N.; Iezzi, G. A Human Self-Locking Cone Morse Connection Retrieved After 30 Years: A Histological and Histomorphometric Case Report. *Eng* **2025**, *6*, 58. https://doi.org/10.3390/eng6030058

Copyright: © 2025 by the authors. Licensee MDPI, Basel, Switzerland. This article is an open access article distributed under the terms and conditions of the Creative Commons Attribution (CC BY) license (https://creativecommons.org/licenses/by/4.0/).

1. Introduction

A comprehensive understanding of bone–implant interface issues require an in-depth examination of biopsies from retrieved human implants, particularly as these are more commonly reported in cases of implant failure, mobility, peri-implantitis, or epithelialization at the interface. Such examinations provide critical insights into the underlying causes and mechanisms of these complications [1]. The literature highlights that dental implants with an intact bone–implant interface are rarely mentioned; instances where implants are retrieved for non-failure reasons, including autopsy, aesthetic concerns, complications

from poor oral hygiene, misalignment affecting functionality or comfort, dysesthesia causing sensory disturbances, or the need for changes in prosthetic protocols, are of primary importance [2–17].

Histological and histomorphometric analyses of stable, functioning osseointegrated implants remain relatively uncommon in the dental literature, especially for implants subjected to prolonged functional loading [18,19]. Functional loading is vital for promoting bone development and maturation as it stimulates remodeling, matrix formation, and adaptation to mechanical stresses, thereby enhancing bone strength and integration [20]. Reports indicate that the duration for which an implant is subjected to functional loading correlates positively with the expected bone-to-implant contact (BIC) [21]. Notably, osseointegration continues to evolve and improve beyond initial full integration, suggesting that the bond between the implant and bone has the potential to strengthen over time [21]. The percentage of BIC (BIC%) is expected to increase due to peri-implant bone remodeling, an ongoing process involving the resorption of old bone and the formation of new bone around the implant, ultimately enhancing integration and stability. This BIC% may continue to improve as the bone adapts to mechanical stresses, thereby contributing to the long-term success and durability of the implant [22,23].

The Cone Morse (CM) implant-abutment junction is designed to optimize the mechanical stability of the implant-abutment connection while simultaneously reducing bacterial infiltration. This is achieved through a "cold fusion" mechanism, which relies on a highly precise conical taper connection between the implant and the abutment. The deep conical interface facilitates a self-locking mechanism that improves screw mechanics by distributing occlusal forces more evenly, thus contributing to long-term marginal bone stability and implant longevity. In contrast, traditional external and internal hex connections often result in micro-gaps that can allow bacterial infiltration, potentially leading to peri-implantitis and soft tissue inflammation, although this topic remains a subject of debate [24,25]. Over the past three decades, the present authors' laboratory has conducted extensive evaluations of numerous retrieved human implants, systematically documenting their performance and outcomes [26–32]. This research has significantly advanced the understanding of their long-term behavior, efficacy, and durability, with some implants experiencing functional loading for several years, including instances lasting over two decades. The detailed case reports resulting from these evaluations have provided invaluable information [33].

The purpose of this case report was to conduct a histological and histomorphometric evaluation of a clinically stable CM conometric implant that was retrieved after over 30 years of functional loading, necessitated by severe bone loss attributed to peri-implantitis and the altered prosthetic requirements of the patient. To the authors' knowledge, this represents the human-retrieved CM implant with the longest documented functional loading period in dental literature.

2. Materials and Methods

2.1. Implant Retrieval and Case Overview

The records from the Implant Retrieval Center at the Dental School of the "G. d'Annunzio" University of Chieti-Pescara in Italy were examined to identify human CM implants that had been extracted after extended periods of loading for non-failure reasons. This review identified a single implant that had been loaded for a duration of 30 years.

This implant featured a self-locking CM conometric connection with a 2.5° taper, a sandblasted and acid-etched surface, and a macro-design characterized by large threads spaced 2 mm apart, along with a reduced transmucosal emergence (MacSystem, Cabon-Denit, Milan, Italy). It was placed in the premolar region of the upper jaw of a 49-year-old patient as part of a dental bridge. The metal-resin composite prosthesis, fab-

ricated 30 years prior, extended from the upper left central incisor (2.1) to the upper left first molar (2.6), with the implant located where the upper left first premolar (2.4) was situated.

Twenty-seven years after the prosthetic rehabilitation, the patient returned to the clinical office. The implant showed stability until its removal three years later, necessitated by the loss of periodontal and bone support related to all adjacent natural teeth, which led to their extraction. Notably, the implant had experienced peri-implantitis for three years, accompanied by a significant peri-implant bone defect. Surgical therapies and surface decontamination were performed twice to address this condition; however, these interventions did not yield favorable results. Furthermore, the continued presence of the implant could potentially compromise the new proposed prosthetic-surgical planning. The implant system used at that time is no longer available on the market, resulting in a shortage of specific prosthetic components.

The actual length of the implant was measured at 12 mm and was used for radiographical calibration. The length originally in bone contact, measured from the top edge of the implant to its tip, was 11 mm. Bone loss was calculated from the calibrated radiograph as the distance between the marginal bone level and the implant apex, totaling 3.5 mm. Importantly, despite the presence of bone pockets surrounding the first thread, due to severe periodontitis affecting neighboring teeth, pre-removal periapical X-rays (Figure 1) also indicated consistent osseointegration of the implant, which was subsequently measured using histological techniques.

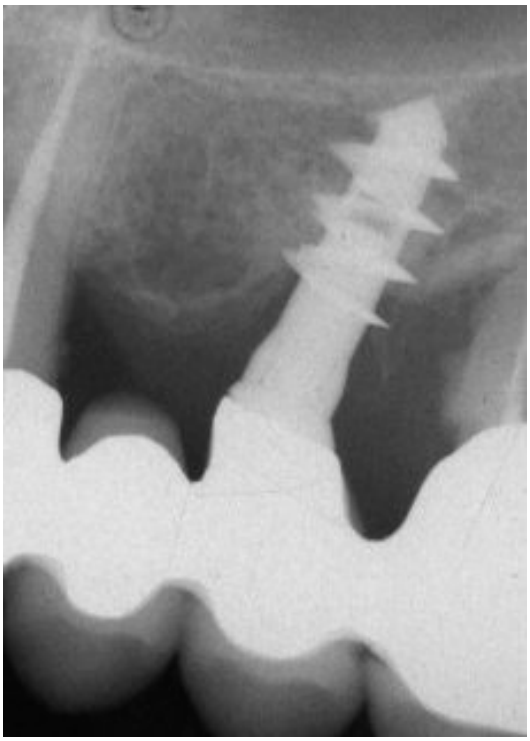

Figure 1. Periapical X-ray before implant retrieval.

Figures 2 and 3 illustrate the case conclusion, featuring an X-ray of the prosthetic rehabilitation after the extraction of the implant and neighboring teeth, along with an image of the completed prosthesis.

The use of this specimen for research purposes was approved by the Ethics Committee of "G. d'Annunzio" University of Chieti-Pescara (CODE: BONEISTO) on 15 September 2019. Informed consent was obtained from the participant. The histological slides were obtained from the laboratory records.

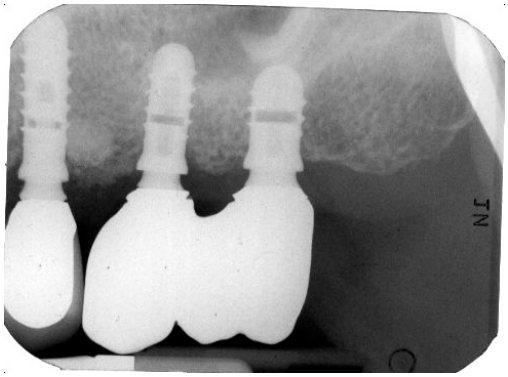

Figure 2. X-ray after the implant retrieval and rehabilitation restoration.

Figure 3. Clinical observation after implant retrieval and rehabilitative restoration.

2.2. Histological Processing and Analysis

The extracted implant and adjacent tissues were immediately preserved in 10% buffered formalin and prepared for thin ground sections [34]. The specimen underwent dehydration through a series of graded alcohol solutions before being embedded in glycolmethacrylate resin. After polymerization, the specimen was cut longitudinally to a thickness of 150 µm along the major axis of the implant, using a high-precision diamond saw, and further ground to an approximate thickness of 30 µm. Two slides were prepared from the central portion of the specimen and stained with acid fuchsin and toluidine blue.

Histomorphometric analysis was carried out to evaluate the average size of osteocyte lacunae and the osteocyte index (*Oi*). The *Oi* was calculated using the following formula:

$$Oi = N.Ot/B.Ar$$

where *N.Ot* represents the number of osteocytes counted at 200× magnification on the section plane for a thin section, and *B.Ar* denotes the total area of the evaluated bone, measured in square micrometers (or square pixels) [35]. The specimens were examined using a transmitted light microscope (Laborlux S, Leitz, Wetzlar, Germany), which was equipped with a high-resolution video camera (3CCD, JVCKY-F55B, JVC, Yokohama, Japan) connected to a monitor and computer (Intel Pentium III 1200 MMX, Intel, Santa Clara, CA, USA). This setup included a digitizing pad and utilized image-capturing software (mvIMPACT v. 3.0, Matrix Vision GmbH, Oppenweiler, Germany). Bone area and cell counts were assessed using image management and analysis software (Image-Pro Plus v. 4.5, Media Cybernetics Inc., Immagini & Computer Snc, Milan, Italy). A single trained examiner (G.I.), who did not participate in the surgical procedure, carried out the histological evaluation.

The images were calibrated using the Pythagorean Theorem to measure distances between selected points in pixels. The BIC% was calculated around the entire perimeter of the implant, accounting for the mineralized bone directly in contact with the implant surface. Additionally, endosseous BIC (EBIC) was evaluated by considering only the endosseous portion of the implant, while the first point of BIC (FBIC) referred to the initial contact of bone with the implant.

2.3. Collagen Fiber Orientation Observed with Polarized Light Microscopy

Birefringence was assessed to determine the orientation of transverse collagen fibers using polarized light. Thin sections of bone were examined under an Axiolab light microscope (Laborlux S, Leitz, Wetzlar, Germany) equipped with two linear polarizers and two quarter-wave plates, allowing for the generation of circularly polarized light. Collagen fibers-oriented perpendicular to the direction of the light (parallel to the plane of the section) appeared bright due to changes in light refraction, while fibers aligned with the axis of the light (perpendicular to the plane of the section) exhibited a spectrum of colors.

2.4. Statistical Analysis

The differences in BIC% and osteocyte density between groups were evaluated using the non-parametric Mann–Whitney U test for independent samples. The results are presented as means ± standard deviation (SD), with a 95% confidence level used for statistical analysis. Additionally, the Spearman rank correlation test was applied to investigate potential correlations between BIC% and osteocyte density.

3. Results

At low magnification, bone tissue was examined in relation to the first or second threads of the implant. The bone displayed a close adherence to the implant surface, with notable density in the areas near the implant body, while the more distant areas contained larger marrow spaces (Figure 4).

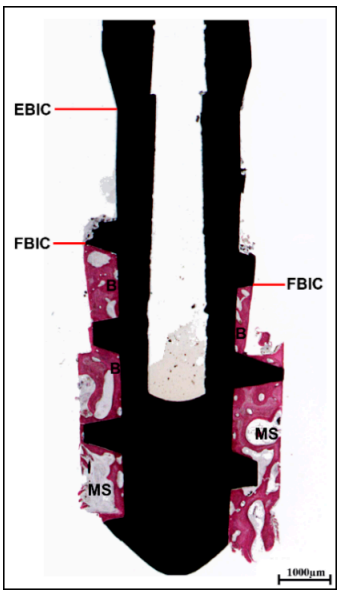

Figure 4. Histological analysis. Presence of bone tissue beginning from the first or second threads of the implant (first bone-to-implant contact: FBIC), rather than from the endosseous portion (endosseous bone-to-implant contact: EBIC). The mature bone (B) in close proximity to the implant surface exhibited a denser structure adjacent to the implant body in contrast to the more distant regions. In the most coronal area, the marrow spaces (MSs) appeared smaller than those in the apical section (acid fuchsin–toluidine blue, magnification 8×).

In the coronal region of the implant, beneath the threads, newly formed bone exhibiting large osteocyte lacunae was observed, indicating a strong affinity for acid fuchsin, a characteristic suggestive of recent bone formation. Bone remodeling was significantly more prominent in this coronal area, likely due to the concentration of occlusal forces. As a result, the dimensions of the osteocyte lacunae were evaluated in both the coronal and apical regions of the implant. The findings revealed that osteocyte lacunae were not only more numerous but also larger in the coronal region compared to the apical region (Figure 5). The Oi and the average area of the osteocyte lacunae are presented in Table 1.

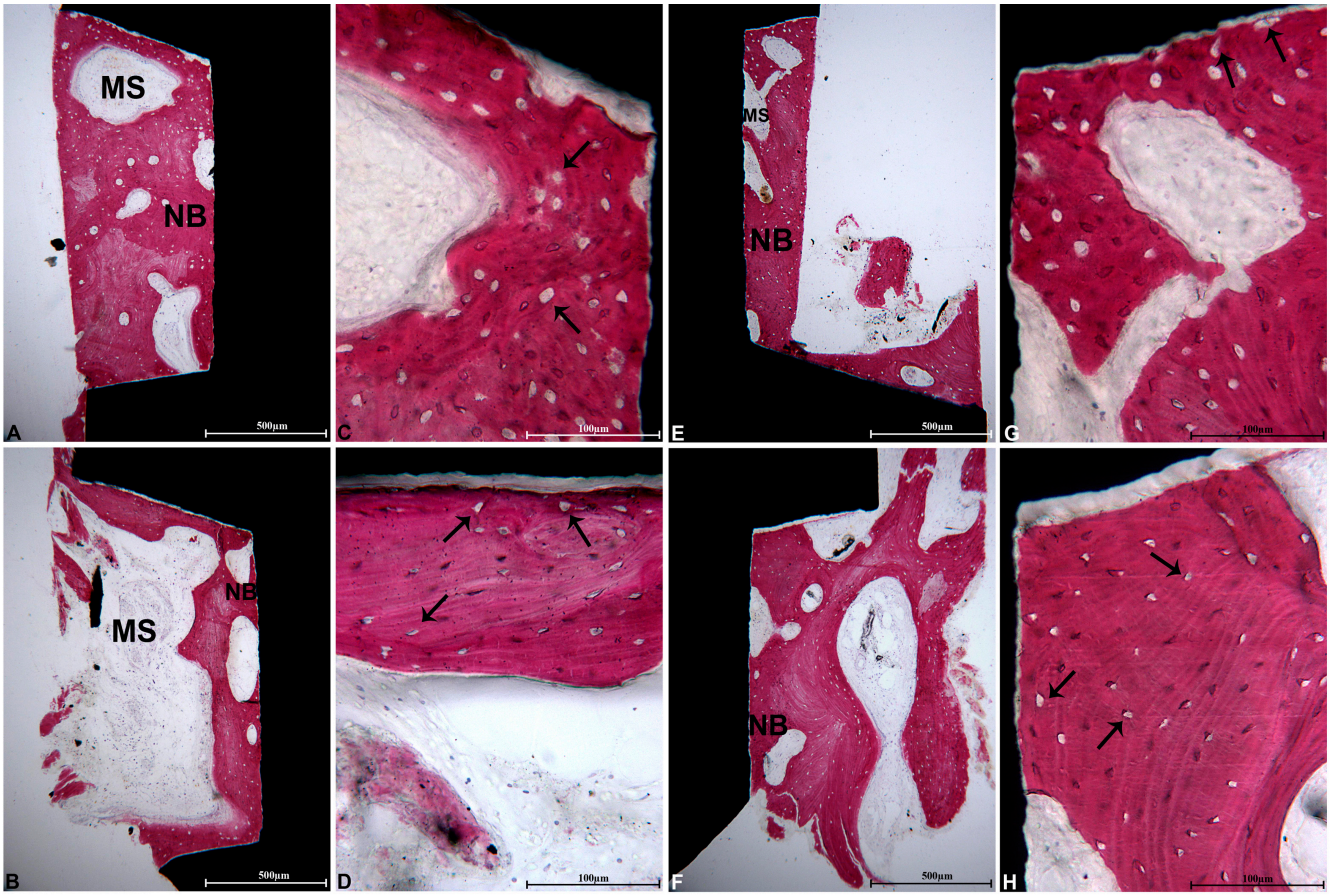

Figure 5. Coronal portion: (**A**) in the initial threads on the right side of the implant, newly formed bone (NB) exhibiting large osteocyte lacunae and MSs was identified. The presence of B was observed at a considerable distance from the interface (acid fuchsin–toluidine blue, magnification 40×); (**C**) at a higher magnification, within the coronal portions beneath the first implant threads, larger osteocyte lacunae were displayed (black arrows) (acid fuchsin–toluidine blue, magnification 200×); (**E**) in the second thread on the left side of the implant, NB exhibiting minimal MSs was located in close proximity to the implant surface (acid fuchsin–toluidine blue, magnification 40×); (**G**) the large osteocyte lacunae (black arrows) were closely associated with the implant surface (acid fuchsin–toluidine blue, magnification 200×). Apical portion: (**B**) in the right section of the implant, NB was in direct contact with the implant surface and demonstrated large MSs (acid fuchsin–toluidine blue, magnification 40×); (**D**) at a higher magnification, the bone beneath the apical threads exhibited smaller osteocyte lacunae compared to those in the coronal portion (black arrows) (acid fuchsin–toluidine blue, magnification 200×); (**F**) in the left portion of the implant, the trabecular bone was also in direct contact with the implant surface (acid fuchsin–toluidine blue, magnification 40×); (**H**) numerous small osteocyte lacunae were noted in proximity to the implant surface (black arrows) (acid fuchsin–toluidine blue, magnification 200×).

Table 1. The average area of osteocyte lacunae and the osteocyte index (Oi) were examined in the coronal and apical regions of the peri-implant bone tissue.

	Average Area of Osteocyte Lacunae (μm^2)	Osteocyte Index (Oi) (#/mm^2)
Coronal Portions	35.290 ± 1.731	736.48 ± 117.695
Apical Portions	16.397 ± 1.362	516.34 ± 21.387
	$p = 0.006$	$p = 0.121$

However, evidence of bone remodeling was observed in several areas, where osteoblasts were actively involved in the deposition of osteoid matrix within the implant threads. Additionally, blood vessels were identified in the marrow spaces adjacent to the osteoblasts. In both the middle and apical regions of the implant, a substantial number of osteons, indicative of a well-organized bone structure, were evident.

Under polarized light examination, the coronal region revealed newly formed bone characterized by collagen fibers that did not exhibit parallel orientation. In contrast, the middle and apical sections displayed lamellar bone, wherein the collagen fibers were oriented parallel to one another (Figure 6).

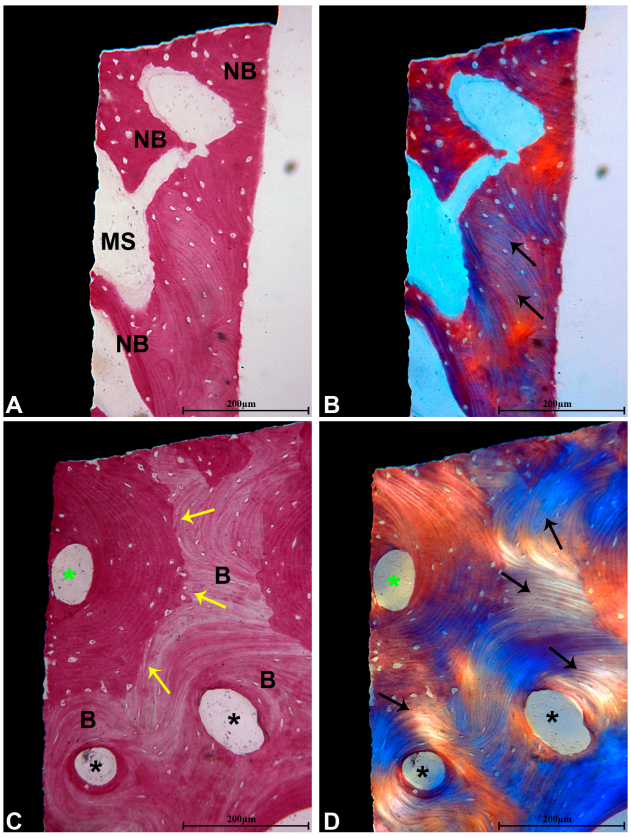

Figure 6. (**A**) Bone remodeling displayed more pronounced activity in the coronal section of the implant, characterized by a higher presence of NB that showed greater staining intensity with acid fuchsin. Small MSs were also observed in close proximity to the implant surface (acid fuchsin–toluidine blue, magnification 100×); (**B**) examination under polarized light revealed only a limited area of bone containing a few collagen fibers oriented in parallel (black arrows), which were not in contact with the implant surface (magnification 100×); (**C**) in the middle and apical segments, B at various maturation stages was present, exhibiting numerous secondary osteons (black *), as well as primary osteon (green *). Reversal lines were also identified between the NB and B (yellow arrows) (acid fuchsin–toluidine blue, magnification 100×); (**D**) under polarized light, lamellar bone featuring parallel-oriented collagen fibers (black arrows) surrounding the osteons (*) was noted (magnification 100×).

The histomorphometric analysis indicated a BIC% of 56.9% ± 0.85 when calculated for the EBIC. Additionally, the BIC was assessed from the FBIC to evaluate BIC independently of crestal bone resorption, which averaged 3.5 mm (Table 2). The discrepancy between EBIC and FBIC was found to be statistically significant (p = 0.00001).

Table 2. The percentage of bone-to-implant contact (BIC%) was determined by considering both the endosseous portion of the implant (EBIC) and the first bone-to-implant contact (FBIC).

	EBIC	**FBIC**
BIC%	56.9 ± 0.85	77.4 ± 0.99

4. Discussion

From a scientific standpoint, the success of dental implant integration is primarily assessed by evaluating the long-term stability of the bone–implant interface and the sustained presence of mineralized tissue at this junction [36–39]. The integrity and functionality of this interface over time reflect the effectiveness of osseointegration and its ability to support prosthetic restorations. Despite comprehensive research in this area, our understanding of the specific mechanisms governing osseointegration in humans remains limited [8]. This knowledge gap highlights the importance of analyzing retrieved human implants, providing valuable insights into the long-term dynamics of osseointegration. Such assessments are vital for optimizing implant design, predicting long-term outcomes, and improving the overall success of dental implant therapies.

Osteocytes, along with osteoblasts and osteoclasts, play a crucial role in regulating bone mass and maintaining structural integrity by coordinating complex processes of bone remodeling and mineralization. Specifically, osteocytes act as mechanosensory and regulatory cells, responding to mechanical stress and metabolic changes. This response directly influences osteoblast-mediated bone formation and osteoclast-driven bone resorption, ensuring a dynamic balance in bone homeostasis [40]. Recent studies have shown that osseointegration is a dynamic and adaptive process, where bone continuously remodels in response to functional loading, improving its mechanical properties over time, particularly in implants subjected to long-term loading [11,21,41]. Bone remodeling is especially pronounced in the coronal regions of implants, where occlusal forces are most concentrated [38]. Functional loading stimulates increased remodeling at the implant interface, leading to a higher proportion of lamellar bone, which is indicative of structural organization and resistance to microdamage [41]. Studies have shown that loaded implants exhibit significantly more newly formed bone at the interface compared to non-loaded implants, reinforcing the idea that active bone remodeling is essential for long-term stability [21,42–44].

This study examined a clinically stable self-locking CM implant, retrieved after over 30 years of functional loading, focusing on its bone–implant interface. The histological and histomorphometric analyses concentrated on measuring the BIC%, tissue responses to functional loading, and the overall structural condition of the interface.

Findings revealed clear evidence of active bone remodeling, particularly in the coronal portion, where osteoblasts actively deposited osteoid matrix within the implant threads. The middle and apical sections displayed a high density of osteons, indicating well-organized bone formation. The first coronal implant thread was subjected to substantially higher mechanical stress due to its proximity to the rigid cortical surface, where greater occlusal forces are transmitted [40,41]. Furthermore, a direct correlation between bone remodeling activity and osteocyte lacunar density was observed, reinforcing prior research from our laboratory. Variations in osteocyte distribution within the lacunae were closely linked to changes in bone remodeling and overall structural integrity [45]. The mechanical

load influenced osteocyte lacunar density, highlighting the adaptive nature of osseointegration in response to sustained functional forces [40,45]. In this study, the average area of osteocyte lacunae was found to be 35.290 ± 1.731 μm^2 in the coronal portions, compared to 16.397 ± 1.362 μm^2 observed in the apical portions (p = 0.006). Additionally, the Oi was significantly elevated in the coronal regions compared to the apical areas, measuring 736.48 ± 117.695 mm^2 versus 516.34 ± 21.387 mm^2 (p = 0.121). Observations under polarized light further indicated that the coronal region exhibited non-parallel collagen fibers, whereas the middle and apical sections were characterized by lamellar bone, multiple secondary osteons, and parallel collagen fiber alignment.

Implants retrieved due to mechanical rather than biological failure are exceptionally rare, providing a valuable opportunity to conduct a comprehensive investigation of the characteristics at the implant–bone interface [11]. As previously noted, various factors can lead to implant removal, including prosthetic complications, misalignment, pain, dysesthesia, hygiene, or psychological factors, despite excellent osseointegration in most cases. The extent of BIC is a key determinant of long-term implant success, with research showing a direct correlation between healing duration and the level of BIC [41]. In this study, the retrieved CM implant, after 30 years of function, exhibited a BIC% of 56.9% ± 0.85 when calculated considering EBIC. The BIC was also derived from the FBIC, which was 77.4% ± 0.99, allowing for an independent assessment of BIC, regardless of crestal bone resorption, which averaged 3.5 mm. These values aligned with long-term findings from the Implant Retrieval Center at the Dental School of the "G. d'Annunzio" University of Chieti-Pescara, Italy, where human-retrieved implants have reported favorable osseointegration and BIC values comparable to this case. For instance, an immediately loaded blade implant inserted into the mandible exhibited a BIC% of 51% ± 6 over a 20-year period [27]. Implants retrieved between 20 and 27 years showed BIC% values ranging from 37.2% to 76% [29]. Furthermore, an analysis of 17 clinically stable and functioning dental implants retrieved over the long term indicated BIC% between 32% ± 4.1 and 83% ± 2.9, following a loading period lasting from 4 to 20 years [30]. Ultimately, a narrative review conducted by our group on a 30-year evaluation of histological and histomorphometric findings on the peri-implant bone in loaded and unloaded dental implants retrieved for various causes confirmed that loaded implants exhibit higher BIC than unloaded ones [46]. This review found compact, lamellar bone with many Haversian systems and osteons near the implant surface with a high BIC% (60–90%) and a significantly higher number of osteocytes and number and thickness of bone trabeculae. In a few implants, a lower BIC%, between 30% and 40%, was observed, with no significant differences in the BIC% of implants retrieved for different reasons. In summary, loading altered the microstructure of the peri-implant bone, and implants were demonstrated to be stable and successful over a wide range of degrees of osseointegration (from 30% to 90%), with loaded implants presenting a 10–12% higher BIC compared to submerged, unloaded implants, and rougher surfaces generally exhibiting about a 10% higher BIC than machined surfaces. Moreover, mineralized bone was not found in unloaded implants at the base of the threads and, in loaded implants, at their tip.

An effective dental implant should have a retentive shape, illustrated by screw-shaped designs. These implants efficiently transmit compressive loads to the surrounding peri-implant bone tissue while creating lower shear stresses at the interface. Sufficient implant stability reduces distortional strains in the newly forming tissues and increases the chances of neo-osteogenesis at the interface. On the other hand, inadequate implant stability may cause significant distortional strain and the development of fibrous tissue at the interface. Primary implant stability and the lack of micromovement are critical factors for the success of dental implants. The macroretention provided by implant threads enhances bone an-

chorage and reduces the risk of implant movement [40]. Moreover, modifications to the implant surface are crucial for promoting BIC and ensuring long-term osseointegration. Traditional surface treatments, like sandblasted, large-grit, acid-etched (SLA) surfaces and anodized titanium oxide layers (TiUnite), have shown substantial improvements in implant stability and bone response. SLA surfaces produce a micro- and nano-textured topography that enhances osteoblast adhesion and supports early bone formation, whereas TiUnite promotes osseointegration through improved surface wettability and better mechanical interlocking due to its thicker oxide layer [47]. Recent innovations, such as hydrophilic modifications (e.g., SLActive), have further refined implant surfaces by reducing protein denaturation and speeding up early healing phases [48]. Additionally, bioactive coatings that include calcium phosphate, nanostructures, or antimicrobial agents have proven effective in enhancing BIC and decreasing peri-implant inflammation [49]. Future research efforts should concentrate on the interactions between these advanced surface treatments and different bone qualities and loading conditions to determine their long-term effectiveness in clinical applications.

The long-term survival of dental implants depends on several factors, including prosthetic design, occlusal loading, and implant surface characteristics. In this case, the metal-resin composite prosthesis made 30 years prior extended from the 2.1 region to the 2.6 region, with the implant located in the 2.4 region. Over time, the natural teeth showed signs of periodontal disease, while the implant developed peri-implantitis, which continued despite repeated interventions. The design of the prosthesis likely led to the uneven distribution of occlusal loads, placing increased biomechanical stress on the implant. Additionally, the surface characteristics of the implant, typical of early-generation models, may have encouraged bacterial adhesion and jeopardized long-term bone stability. Occlusal overloading, alongside progressive bone loss and inflammation, can expedite peri-implant disease and threaten implant longevity. Ultimately, the condition and position of the implant became incompatible with the new implant-prosthetic rehabilitation plan, forcing its removal after three decades of functionality. These findings underscored the critical importance of prosthetic planning, load management, and advanced surface treatments in ensuring the long-term success of implant-supported restorations. When interpreting the results and assessing the broader applicability of the self-locking CM implant in clinical practice, it is essential to acknowledge several limitations. The study consisted of a single-case analysis of only one retrieved implant, which may limit generalizability. Furthermore, it lacked comparative data with other types of implants or abutment connections and focused solely on BIC without considering additional factors such as bone density. Additionally, the retrieval was conducted from one single patient after more than 30 years, raising potential bias concerns. The examination offers only a snapshot of the implant's condition, failing to account for potential changes over time and neglecting to address possible long-term effects beyond the 30-year mark. Lastly, there may be limitations in detecting subtle differences in bone–implant integration due to the histological methods used. Nonetheless, these findings confirmed that the self-locking CM design effectively guarantees durable and successful osseointegration in clinical applications. The CM implant-abutment junction represents a significant advancement in the field of implantology, providing superior mechanical retention, bacterial resistance, and long-term bone preservation. The cold-fusion effect promotes a highly stable and secure connection, ultimately enhancing the predictability and success of dental implant restorations [50]. There were no reported cases of epithelial migration, inflammatory infiltration, or fibrous tissue at the interface, indicating that this type of implant can offer long-term stability and integration. To the authors' knowledge, this is the longest-documented functional loading period for a human implant in the dental literature.

Positioning these implant-abutment junctions subcrestally has been linked to reduced or no peri-implant bone resorption. The need for a more apical placement of the micro-gap is mainly associated with achieving an enhanced and aesthetically pleasing prosthetic emergence profile, which minimizes the risk of exposing the implant threads [51,52]. Future studies involving clinical cases or numerical simulations using the finite element method can help investigate the effects of placing CM dental implants at equicrestal and subcrestal levels on load distribution and BIC% under functional loading over extended periods. This could help define an approach that is recommended to minimize peri-implant bone resorption and ensure long-term implant success [53].

Author Contributions: Conceptualization, C.M., A.P. and F.G.M.; methodology, C.M., N.D.P. and G.I.; software, C.M., G.I. and M.T.; validation, C.M., N.D.P. and G.I.; formal analysis, T.R., N.D.P. and G.I.; investigation, C.M. and M.T.; resources, C.M., N.D.P. and G.I.; data curation, F.G.M., T.R. and G.I.; writing—original draft preparation, A.P. and G.I.; writing—review and editing, M.T. and T.R.; visualization, M.T. and T.R.; supervision, N.D.P. and G.I.; project administration, C.M., A.P., N.D.P. and G.I.; funding acquisition, C.M., N.D.P. and G.I. All authors have read and agreed to the published version of the manuscript.

Funding: This research received no external funding.

Institutional Review Board Statement: The study was conducted in accordance with the Declaration of Helsinki and approved by the Ethics Committee of "G. d'Annunzio" UNIVERSITY OF CHIETI-PESCARA (protocol code BONEISTO, 15 September 2019).

Informed Consent Statement: Informed consent was obtained from all subjects involved in the study.

Data Availability Statement: The original contributions presented in this study are included in the article. Further inquiries can be directed to the corresponding author.

Conflicts of Interest: The authors declare no conflicts of interest.

Abbreviations

The following abbreviations are used in this manuscript:

BIC	Bone-to-implant contact
CM	Cone Morse
Oi	Osteocyte index
N.Ot	Number of osteocytes
B.Ar	Total area of the bone
FBIC	First bone-to-implant contact
EBIC	Endosseous bone-to-implant contact
B	Mature bone
MSs	Marrow spaces
NB	Newly formed bone

References

1. Piattelli, A.; Scarano, A.; Piattelli, M. Histologic observations on 230 retrieved dental implants: 8 years' experience (1989–1996). *J. Periodontol.* **1998**, *69*, 178–184. [CrossRef] [PubMed]
2. Sennerby, L.; Ericson, L.E.; Thomsen, P.; Lekholm, U.; Åstrand, P. Structure of the bone-titanium interface in retrieved clinical oral implants. *Clin. Oral Implant. Res.* **1991**, *2*, 103–111. [CrossRef] [PubMed]
3. Donath, K. Pathogenesis of bony pocket formation around dental implants. *J. Dent. Assoc. South Afr. Tydskr. Tandheelkd. Ver. Van Suid-Afr.* **1992**, *47*, 204–208.
4. Albrektsson, T.; Eriksson, A.R.; Friberg, B.; Lekholm, U.; Lindahl, L.; Nevins, M.; Oikarinen, V.; Roos, J.; Sennerby, L.; Astrand, P. Histologic investigations on 33 retrieved nobelpharma implants. *Clin. Mater.* **1993**, *12*, 1–9. [CrossRef]

5. Steflik, D.E.; Corpe, R.S.; Young, T.R.; Parr, G.R.; Tucker, M.; Sims, M.; Tinley, J.; Sisk, A.; McDaniel, M. Light microscopic and scanning electron microscopic retrieval analyses of implanted biomaterials retrieved from humans and experimental animals. *J. Oral Implantol.* **2001**, *27*, 5–15. [CrossRef]
6. Bolind, P.K.; Johansson, C.B.; Becker, W.; Langer, L.; Sevetz, E.B.; Albrektsson, T.O. A descriptive study on retrieved non-threaded and threaded implant designs. *Clin. Oral Implant. Res.* **2005**, *16*, 447–455. [CrossRef]
7. Lemons, J.; Brott, B.; Eberhardt, A. Human postmortem device retrieval and analysisorthopaedic, cardiovascular, and dental systems. *J. Long Term Eff. Med. Implant* **2010**, *20*, 81–85. [CrossRef]
8. Kim, Y.K.; Kim, S.G.; Kim, J.Y.; Heo, Y.K.; Park, J.C.; Oh, J.S. Histologic evaluation of a retrieved endosseous implant: A case report. *Int. J. Periodontics Restor. Dent.* **2013**, *33*, e32–e36. [CrossRef]
9. Laursen, M.G.; Melsen, B.; Cattaneo, P.M. An evaluation of insertion sites for mini-implants. *Angle Orthod.* **2013**, *83*, 222–229. [CrossRef]
10. Nordquist, W.D.; Krutchkoff, D.J. The custom endosteal implant: Histology and case report of a retrieved maxillary custom osseous-integrated implant nine years in service. *J. Oral Implantol.* **2014**, *40*, 195–201. [CrossRef]
11. Shah, F.A.; Nilson, B.; Brånemark, R.; Thomsen, P.; Palmquist, A. The bone-implant interface—nanoscale analysis of clinically retrieved dental implants. *Nanomed. Nanotechnol. Biol. Med.* **2014**, *10*, 1729–1737. [CrossRef]
12. Kohal, R.; Schwindling, F.S.; Bächle, M.; Spies, B.C. Peri-implant bone response to retrieved human zirconia oral implants after a 4-year loading period: A histologic and histomorphometric evaluation of 22 cases. *J. Biomed. Mater. Res.* **2016**, *104*, 1622–1631. [CrossRef] [PubMed]
13. Piattelli, A.; Trisi, P.; Romasco, N.; Emanuelli, M. Histologic analysis of a screw implant retrieved from man: Influence of early loading and primary stability. *J. Oral Implantol.* **1993**, *19*, 303–306. [PubMed]
14. Piattelli, A.; Scarano, A.; Piattelli, M.; Bertolai, R.; Panzoni, E. Histologic aspects of the bone and soft tissues surrounding three titanium non-submerged plasma-sprayed implants retrieved at autopsy: A case report. *J. Periodontol.* **1997**, *68*, 694–700. [CrossRef] [PubMed]
15. Orsini, G.; Fanali, S.; Scarano, A.; Petrone, G.; di Silvestro, S.; Piattelli, A. Tissue reactions, fluids, and bacterial infiltration in implants retrieved at autopsy: A case report. *Int. J. Oral Maxillofac. Implant.* **2000**, *15*, 283–286.
16. Romanos, G.E.; Traini, T.; Johansson, C.B.; Piattelli, A. Biologic width and morphologic characteristics of soft tissues around immediately loaded implants: Studies performed on human autopsy specimens. *J. Periodontol.* **2010**, *81*, 70–78. [CrossRef]
17. Iezzi, G.; Vantaggiato, G.; Shibli, J.A.; Fiera, E.; Falco, A.; Piattelli, A.; Perrotti, V. Machined and sandblasted human dental implants retrieved after 5 years: A histologic and histomorphometric analysis of three cases. *Quintessence Int.* **2012**, *43*, 287–292.
18. Lederman, P.D.; Schenk, R.K.; Buser, D. Long-lasting osseointegration of immediately loaded, bar-connected TPS screws after 12 years of function: A histologic case report of a 95-year-old patient. *Int. J. Periodontics Restor. Dent.* **1998**, *18*, 552.
19. Cappuccilli, M.; Conte, M.; Praiss, S.T. Placement and post-mortem retrieval of a 28-year-old implant: A clinical and histologic report. *J. Am. Dent. Assoc.* **2004**, *135*, 324–329. [CrossRef]
20. Coelho, P.G.; Bonfante, E.A.; Marin, C.; Granato, R.; Giro, G.; Suzuki, M. A human retrieval study of plasma-sprayed hydroxyapatite-coated plateau root form implants after 2 months to 13 years in function. *J. Long Term Eff. Med. Implant.* **2010**, *20*, 335–342. [CrossRef]
21. Gil, L.F.; Suzuki, M.; Janal, M.N.; Tovar, N.; Marin, C.; Granato, R.; Bonfante, E.A.; Jimbo, R.; Gil, J.N.; Coelho, P.G. Progressive plateau root form dental implant osseointegration: A human retrieval study. *J. Biomed. Mater. Res.* **2015**, *103*, 1328–1332. [CrossRef]
22. Proussaefs, P.T.; Tatakis, D.N.; Lozada, J.; Caplanis, N.; Rohrer, M.D. Histologic evaluation of hydroxyapatite-coated root-form implants retrieved after 7 years in function: A case report. *Int. J. Oral Maxillofac. Implant.* **2000**, *15*, 438.
23. Proussaefs, P.; Lozada, J. Histologic evaluation of a 9-year-old hydroxyapatite-coated cylindric implant placed in conjunction with a subantral augmentation procedure: A case report. *Int. J. Oral Maxillofac. Implant.* **2001**, *16*, 737–741.
24. Ardakani, M.R.T.; Meimandi, M.; Amid, R.; Pourahmadie, A.D.; Shidfar, S. In vitro comparison of microbial leakage of the implant-healing abutment interface in four connection systems. *J. Oral Implantol.* **2019**, *45*, 350–355. [CrossRef] [PubMed]
25. Mihali, S.G.; Wang, H.L.; Karancsi, O.; Bratu, E.A. Internal hexagon vs conical implant-abutment connections: Evaluation of 3-year postloading outcomes. *J. Oral Implantol.* **2021**, *47*, 485–490. [CrossRef]
26. Piattelli, A.; Scarano, A.; Paolantonio, M. Immediately loaded screw implant removed for fracture after a 15-year loading period: Histological and histochemical analysis. *J. Oral Implantol.* **1997**, *1*, 75–79.
27. Stefano, D.D.; Iezzi, G.; Scarano, A.; Perrotti, V.; Piattelli, A. Immediately loaded blade implant retrieved from a man after a 20-year loading period: A histologic and histomorphometric case report. *J. Oral Implantol.* **2006**, *32*, 171–176. [CrossRef]
28. Iezzi, G.; Scarano, A.; Petrone, G.; Piattelli, A. Two human hydroxyapatite-coated dental implants retrieved after a 14-year loading period: A histologic and histomorphometric case report. *J. Periodontol.* **2007**, *78*, 940–947. [CrossRef]
29. Mangano, C.; Piattelli, A.; Mortellaro, C.; Mangano, F.; Perrotti, V.; Iezzi, G. Evaluation of peri-implant bone response in implants retrieved for fracture after more than 20 years of loading: A case series. *J. Oral Implantol.* **2015**, *41*, 414–418. [CrossRef]

30. Iezzi, G.; Piattelli, A.; Mangano, C.; Degidi, M.; Testori, T.; Vantaggiato, G.; Fiera, E.; Frosecchi, M.; Floris, P.; Perroni, R.; et al. Periimplant bone response in human-retrieved, clinically stable, successful, and functioning dental implants after a long-term loading period: A report of 17 cases from 4 to 20 years. *Implant. Dent.* **2016**, *25*, 380–386. [CrossRef]
31. Iezzi, G.; Degidi, M.; Shibli, J.; Vantaggiato, G.; Piattelli, A.; Perrotti, V. Bone response to dental implants after a 3- to 10-year loading period: A histologic and histomorphometric report of four cases. *Int. J. Periodontics Restor. Dent.* **2013**, *33*, 755–761. [CrossRef] [PubMed]
32. Degidi, M.; Perrotti, V.; Shibli, J.A.; Mortellaro, C.; Piattelli, A.; Iezzi, G. Evaluation of the peri-implant bone around parallel-walled dental implants with a condensing thread macrodesign and a self-tapping apex: A 10-year retrospective histological analysis. *J. Craniofacial Surg.* **2014**, *25*, 840–842. [CrossRef]
33. Sarve, H.; Friberg, B.; Borgefors, G.; Johansson, C.B. Introducing a novel analysis technique for osseointegrated dental implants retrieved 29 years postsurgery. *Clin. Implant. Dent. Rel. Res.* **2013**, *15*, 538–549. [CrossRef] [PubMed]
34. Piattelli, A.; Scarano, A.; Quaranta, M. High-precision, cost-effective cutting system for producing thin sections of oral tissues containing dental implants. *Biomaterials* **1997**, *18*, 577–579. [CrossRef] [PubMed]
35. Piattelli, A.; Artese, L.; Penitente, E.; Iaculli, F.; Degidi, M.; Mangano, C.; Shibli, J.A.; Coelho, P.G.; Perrotti, V.; Iezzi, G. Osteocyte density in the peri-implant bone of implants retrieved after different time periods (4 weeks to 27 years). *J. Biomed. Mater. Res. B Appl. Biomater.* **2014**, *102*, 239–243. [CrossRef]
36. Martin, R.B.; Boardman, D.L. The Effects of Collagen Fiber Orientation, Porosity, Density, and Mineralization on Bovine Cortical Bone Bending Properties. *J. Biomech.* **1993**, *26*, 1047–1054. [CrossRef]
37. Linkow, L.I.; Donath, K.; Lemons, J.E. retrieval analyses of a blade implant after 231 months of clinical function. *Implant. Dent.* **1992**, *1*, 27–48. [CrossRef]
38. Proussaefs, P.; Lozada, J. Evaluation of two vitallium blade-form implants retrieved after 13 to 21 years of function: A clinical report. *J. Prosthet. Dent.* **2002**, *87*, 412–415. [CrossRef]
39. Abbott, J.R.; Marino, V.; Bartold, P.M. Human cadaveric histomorphological and metallurgical analysis of dental implants following 12.5 years of service. *Clin. Oral Implant. Res.* **2014**, *25*, 266–271. [CrossRef] [PubMed]
40. Delgado-Ruiz, R.A.; Calvo-Guirado, J.L.; Romanos, G.E. Effects of occlusal forces on the peri-implant-bone interface stability. *Periodontology 2000* **2019**, *81*, 179–193. [CrossRef]
41. Coelho, P.G.; Suzuki, M.; Marin, C.; Granato, R.; Gil, L.F.; Tovar, N.; Jimbo, R.; Neiva, R.; Bonfante, E.A. Osseointegration of plateau root form implants: Unique healing pathway leading to haversian-like long-term morphology. In *Engineering Mineralized and Load Bearing Tissues*; Bertassoni, L.E., Coelho, P.G., Eds.; Advances in Experimental Medicine and Biology; Springer International Publishing: Cham, Switzerland, 2015; Volume 881, pp. 111–128. ISBN 978-3-319-22344-5.
42. Degidi, M.; Scarano, A.; Iezzi, G.; Piattelli, A. Histologic analysis of an immediately loaded implant retrieved after 2 months. *J. Oral Implantol.* **2005**, *31*, 247–254. [CrossRef] [PubMed]
43. De Calais, C.D.; Bordin, D.; Piattelli, A.; Iezzi, G.; Negretto, A.; Shibli, J.A. Lateral static overload on immediately restored implants decreases the osteocyte index in peri-implant bone: A secondary analysis of a pre-clinical study in dogs. *Clin. Oral Investig.* **2021**, *25*, 3297–3303. [CrossRef]
44. Insua, A.; Monje, A.; Wang, H.L.; Miron, R.J. Basis of bone metabolism around dental implants during osseointegration and peri-implant bone loss. *J. Biomed. Mater. Res. A* **2017**, *105*, 2075–2089. [CrossRef] [PubMed]
45. Iezzi, G.; Mangano, C.; Barone, A.; Tirone, F.; Baggi, L.; Tromba, G.; Piattelli, A.; Giuliani, A. Jawbone remodeling: A conceptual study based on synchrotron high-resolution tomography. *Sci. Rep.* **2020**, *10*, 3777. [CrossRef]
46. Tumedei, M.; Piattelli, A.; Degidi, M.; Mangano, C.; Iezzi, G. A narrative review of the histological and histomorphometrical evaluation of the peri-implant bone in loaded and unloaded dental implants. A 30-year experience (1988–2018). *Int. J. Environ. Res. Public Health* **2020**, *17*, 2088. [CrossRef]
47. Smeets, R.; Stadlinger, B.; Schwarz, F.; Beck-Broichsitter, B.; Jung, O.; Precht, C.; Kloss, F.; Gröbe, A.; Heiland, M.; Ebker, T. Impact of dental implant surface modifications on osseointegration. *Biomed. Res. Int.* **2016**, *2016*, 6285620. [CrossRef] [PubMed]
48. Wennerberg, A.; Galli, S.; Albrektsson, T. Current knowledge about the hydrophilic and nanostructured SLActive surface. *Clin. Cosmet. Investig. Dent.* **2011**, *3*, 59–67. [CrossRef]
49. Kulkarni Aranya, A.; Pushalkar, S.; Zhao, M.; LeGeros, R.Z.; Zhang, Y.; Saxena, D. Antibacterial and bioactive coatings on titanium implant surfaces. *J. Biomed. Mater. Res. A* **2017**, *105*, 2218–2227. [CrossRef]
50. Vinhas, A.S.; Aroso, C.; Salazar, F.; López-Jarana, P.; Ríos-Santos, J.V.; Herrero-Climent, M. Review of the mechanical behavior of different implant–abutment connections. *Int. J. Environ. Res. Public Health.* **2020**, *17*, 8685. [CrossRef]
51. Degidi, M.; Nardi, D.; Daprile, G.; Piattelli, A. Nonremoval of immediate abutments in cases involving subcrestally placed postextractive tapered single implants: A randomized controlled clinical study. *Clin. Implant. Dent. Relat. Res.* **2014**, *16*, 794–805. [CrossRef]

52. Fetner, M.; Fetner, A.; Koutouzis, T.; Clozza, E.; Tovar, N.; Sarendranath, A.; Coelho, P.; Neiva, K.; Janal, M.; Neiva, R. The effects of subcrestal implant placement on crestal bone levels and bone-to-abutment contact: A microcomputed tomographic and histologic study in dogs. *Int. J. Oral Maxillofac. Implant.* **2015**, *30*, 1068–1075. [CrossRef] [PubMed]
53. Comuzzi, L.; Ceddia, M.; Di Pietro, N.; Inchingolo, F.; Inchingolo, A.M.; Romasco, T.; Tumedei, M.; Specchiulli, A.; Piattelli, A.; Trentadue, B. Crestal and subcrestal placement of morse cone implant-abutment connection implants: An in vitro finite element analysis (FEA) study. *Biomedicines* **2023**, *11*, 3077. [CrossRef] [PubMed]

Disclaimer/Publisher's Note: The statements, opinions and data contained in all publications are solely those of the individual author(s) and contributor(s) and not of MDPI and/or the editor(s). MDPI and/or the editor(s) disclaim responsibility for any injury to people or property resulting from any ideas, methods, instructions or products referred to in the content.